On the flux linkage between pancake coils in resonance-type wireless power transfer systems

Mauro Parise, Daniele Romano, and Giulio Antonini

Abstract

This work presents a series representation for the mutual inductance of two co-axial pancake coils which remains accurate in non-quasi-static regime under the hypothesis that the current in the source coil is uniformly distributed. Making use of the Gegenbauer's addition theorem, and a term-by-term analytical integration, the mutual inductance between two generic turns belonging to distinct coils is expressed as a sum of spherical Hankel functions with algebraic coefficients. The accuracy and efficiency of the resulting expression is proved through pertinent numerical examples.

Index Terms

Loop antennas, magnetic resonance imaging, flux linkage, surface coils.

I. Introduction

In the last decades, wireless power transfer (WPT) systems have attracted the interest of researchers working in a variety of scientific fields [1]–[8]. In fact, WPT systems find application in automotive battery [1] and consumer electronics' charging [2], in pacemaker battery charging [3], and in inductive links for low-power three-dimensional (3-D) integration systems [4]. Among all the WPT technologies, magnetic resonance coupling (MRC) method is the one that offers better performances in terms of transfer distance and efficiency. In particular, previous authors have experimentally shown that efficiency of MRC-WPT is still reasonable even if transfer distances is slightly less than 10 times the radius of the coils [5], [6].

In the past years, an analytical formula has been presented that allows to predict the magnetic coupling of two co-axial circular pancake coils [9]. However, the derived expression for the mutual inductance has the disadvantage of being in integral form and, what is more, of being tailored to the quasi-static frequency range only. As such, it can be used only if the effects of the displacement currents are negligible. Hence, when the operating frequency exceeds a few tens of MHz, like in ISM Band applications, the overall size of the whole two-coil system may not be any longer small enough for electromagnetic retardation to have negligible effect on the field distribution, and the quasi-static approximation fails.

The scope of this work is to derive a series representation for the mutual inductance of two co-axial pancake coils, which is valid in both the quasi-static and non-quasi-static frequency ranges of the two-coil system, provided that the current in the source coil may be assumed to be uniformly distributed. This occurs up to the frequency at which the length of the wire that constitutes the coil is approximately one third of the free-space wavelength [10]. The expression comes from applying the integral form of Gegenbauer's addition theorem to the semi-infinite integral representation for the mutual inductance between two generic turns belonging to distinct coils. This permits to convert the product of Bessel functions of the integrand into the finite integral of a single Bessel function. Next, the semi-infinite integration is carried out analytically, and the integrand of the remaining finite integral is expanded into a power series of the cosine of the integration variable. This makes it possible to perform term-by-term analytical integration, and express the mutual inductance as a sum of spherical Hankel functions with

Manuscript received October 6, 2019.

Mauro Parise is with the Unit of Electrical Engineering, University Campus Bio-Medico of Rome, Via Alvaro del Portillo 21, 00128 Rome, Italy, email: m.parise@unicampus.it

Daniele Romano and Giulio Antonini are with the UAq EMC Laboratory, Dipartimento di Ingegneria Industriale e dell'Informazione e di Economia, Università degli Studi dell'Aquila, Via G. Gronchi 18, 67100, L'Aquila, Italy, e-mail: giulio.antonini@univaq.it.

algebraic coefficients. The obtained formula holds as long as the thin-wire assumption, underlying the present derivation, is valid. This means that the wire radius must be far smaller than the radii of the turns that constitute the pancake coils. The advantages of the derived expression in terms of accuracy and time cost are illustrated through numerical examples.

II. Theory

Consider two thin-wire air-cored coaxial pancake coils separated by the distance d, as shown in Fig. 1. If we denote by a_i $(i = 1, \ldots, N_a)$ the radii of the turns of the lower coil, and by b_j $(j = 1, \ldots, N_b)$ the radii of the turns of the upper coil, the flux linkage per unit current between the coils may be expressed as

$$M_{tot} = \sum_{i=1}^{N_a} \sum_{j=1}^{N_b} M(a_i, b_j), \tag{1}$$

where $M(a, b)$ is the mutual inductance of two generic turns with radii a and b.

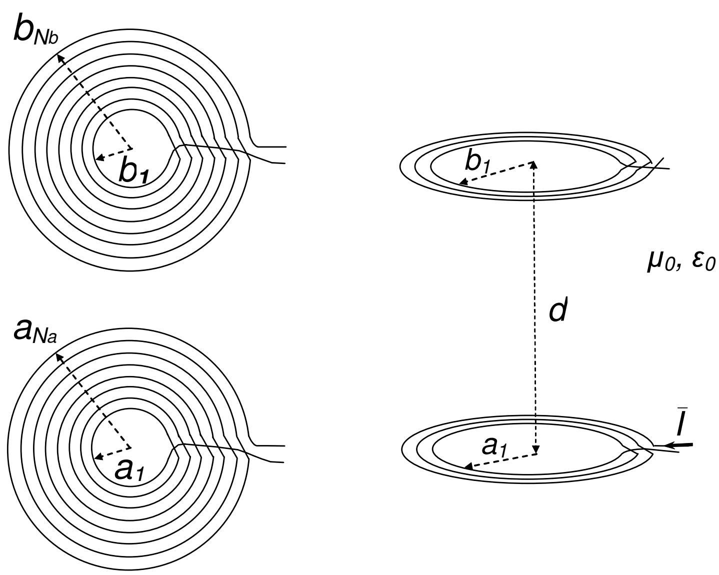

Fig. 1: Sketch of two coaxial pancake coils.

The purpose of this section is to exactly evaluate the complete integral representation for $M(a, b)$, given by [9]

$$M(a, b) = \pi\mu_0 ab \int_0^\infty \frac{e^{-u_0 d}}{u_0} J_1(k_\rho a)\, J_1(k_\rho b) k_\rho \, dk_\rho, \tag{2}$$

being $J_\nu(\cdot)$ the νth-order Bessel function, and

$$u_0 = \sqrt{k_\rho^2 - k_0^2}, \qquad k_0^2 = \omega^2 \mu_0 \epsilon_0, \tag{3}$$

where μ_0 and ϵ_0 are, respectively, the magnetic permeability and dielectric permittivity of free space. To accomplish this task, we first use the relation [11, 11.41.17]

$$J_1(k_\rho a)\, J_1(k_\rho b) = \frac{1}{\pi} \int_0^\pi J_0(k_\rho q)\, \cos\phi \, d\phi, \tag{4}$$

with

$$q = \sqrt{a^2 + b^2 - 2ab\cos\phi}, \tag{5}$$

so as to express (2) as

$$M(a,b)=\mu_0 ab\int_0^{\pi}\cos\phi\left[\int_0^{\infty}\frac{e^{-u_0 d}}{u_0}J_0\left(k_\rho q\right)k_\rho dk_\rho\right]d\phi. \tag{6}$$

Sommerfeld Identity can now be applied to the evaluation of the improper integral within the square brackets of (6). It reads [12, p. 9, no. 24]

$$\begin{aligned}\int_0^{\infty}\frac{e^{-u_0 d}}{u_0}J_0(k_\rho q)k_\rho dk_\rho &= \frac{e^{-jk_0\sqrt{q^2+d^2}}}{\sqrt{q^2+d^2}}\\ &= -jk_0 h_0^{(2)}\left(k_0\sqrt{q^2+d^2}\right),\end{aligned} \tag{7}$$

where $h_l^{(2)}\left(\xi\right)$ is the lth-order spherical Hankel function of the second kind, and (7) is thus turned into

$$M(a,b)=-j\mu_0 k_0 ab\int_0^{\pi}g_0\left(k_0\sqrt{q^2+d^2}\right)\cos\phi\, d\phi. \tag{8}$$

with

$$g_n\left(\xi\right)=\frac{h_n^{(2)}\left(\xi\right)}{\xi^n}. \tag{9}$$

Upon setting

$$r^2=a^2+b^2+d^2, \tag{10}$$

equation (8) may be rewritten as

$$M(a,b)=-j\mu_0 k_0 ab\int_0^{\pi}g_0\left(k_0\sqrt{r^2+\tau}\right)\cos\phi\, d\phi, \tag{11}$$

being $\tau=-2ab\cos\phi$, and the analytical evaluation of the finite integral may be carried out once g_0, seen as a function of τ, is replaced with its Maclaurin expansion. It yields [13]

$$g_0\left(k_0\sqrt{r^2+\tau}\right)=\sum_{n=0}^{\infty}\frac{1}{n!}\left(-\frac{k_0^2\tau}{2}\right)^n g_n\left(k_0 r\right), \tag{12}$$

and (8) becomes

$$M(a,b)=-j\mu_0 k_0 ab\sum_{n=0}^{\infty}\frac{\left(k_0^2 ab\right)^n}{n!}g_n\left(k_0 r\right)\int_0^{\pi}\cos^{n+1}\phi\, d\phi. \tag{13}$$

Finally, use the tabulated result [14, 2.512.2-2.512.3]

$$\int_0^{\pi}\cos^{n+1}\phi=\begin{cases}\pi\, n!!\,/(n+1)!!, & \text{odd } n\\ 0, & \text{even } n\end{cases} \tag{14}$$

makes it possible to obtain

$$M(a,b)=-j\pi\mu_0 k_0 ab\sum_{l=0}^{\infty}\frac{1}{2^{2l+1}l!(l+1)!}\left(\frac{k_0 ab}{r}\right)^{2l+1}h_{2l+1}^{(2)}\left(k_0 r\right), \tag{15}$$

where account has been taken of (9). A simplified expression for $M(a,b)$ may be obtained under the small-loop assumption, that is by setting $a\rightarrow 0$ and $b\rightarrow 0$. This means retaining only the first term (l=0) of the sum in (15), and letting $r\rightarrow d$. It yields

$$M(a,b)=-\frac{j\pi\mu_0\left(k_0 ab\right)^2}{2d}h_1^{(2)}\left(k_0 d\right), \tag{16}$$

and, after substituting the following identity [15]–[19]

$$h_l^{(2)}\left(k_0 d\right)=j^{l+1}\frac{e^{-jk_0 d}}{k_0 d}\sum_{i=0}^{l}\frac{(l+i)!}{i!(l-i)!}\left(2jk_0 d\right)^{-i}, \tag{17}$$

one obtains

$$M(a,b)=\frac{j\pi\mu_0 k_0}{2}\left(\frac{ab}{d}\right)^2\left(1+\frac{1}{jk_0 d}\right)e^{-jk_0 d}. \tag{18}$$

III. Numerical results

As validation, the developed theory is applied to the computation of the amplitude of the mutual inductance between two coils made up of three turns, with radii a_1=b_1=4 cm, a_2=b_2=6 cm, and a_3=b_3=8 cm. At first, the coil-to-coil spacing is assumed to be d=10 cm, and the inductance is computed against frequency by using (1) in conjunction with (15), numerical integration of (2), and the well-known quasi-static solution in terms of complete Elliptic Integrals in [9]. In particular, numerical integration is performed by applying a G7-K15 Gauss-Kronrod quadrature scheme, arising from combining a 7-point Gauss rule with a 15-point Kronrod rule, while (15) is truncated at the index L, which is taken as a parameter. The obtained results, depicted in Fig. 2, point out how the outcomes from the G7-K15 scheme perfectly agree with those resulting from (15) with L=4. Instead, the quasi-static formula does not depend on frequency and, as a consequence, can generate accurate results only in the low-frequency range, up to less than 10 MHz. Thereinafter, the whole two-coil system enters its non-quasi-static frequency region, where the effects of the displacement currents cease to be negligible. Thus, starting from about 10 MHz the system is no longer small enough for electromagnetic retardation to have negligible effect on the field distribution. A glance at the curves plotted in Fig. 2 also allows to conclude that expression (15) for the

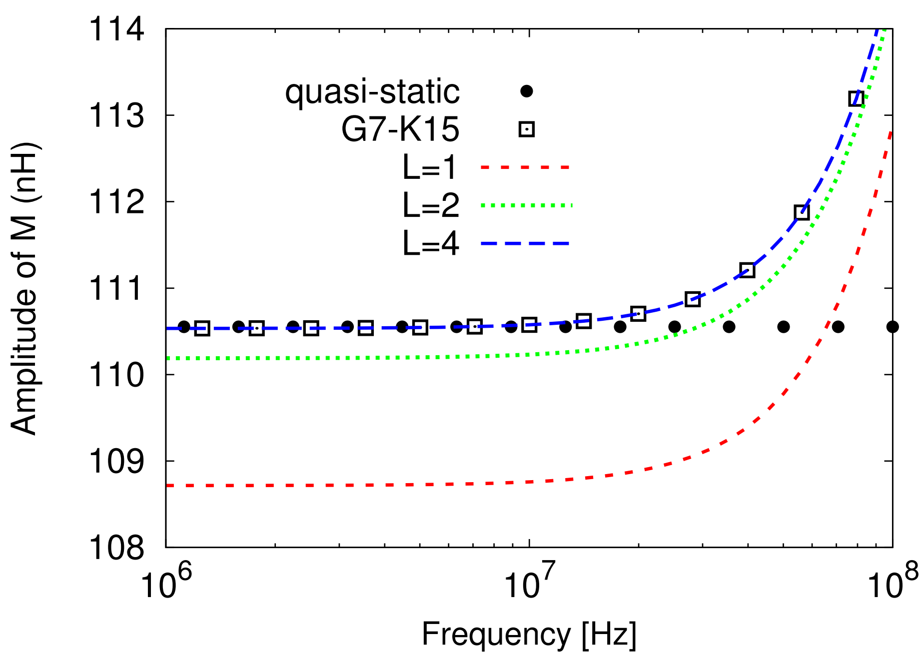

Fig. 2: Mutual inductance between two pancake coils separated by the distance d=10 cm, calculated versus frequency.

mutual inductance converges to the exact solution regardless of the operating frequency. Thus, if M is the exact value of the inductance at a given frequency, and $\{M_L\}$ is the sequence of partial sums that originates from truncating (15) at the index L, it holds [20]

$$\lim_{L\to\infty}\frac{|M_{L+1}-M|}{|M_L-M|^{\delta}}=c, \tag{19}$$

where $\delta \geq 1$ and c are, respectively, the order of convergence (OC) and the asymptotic error constant (AEC), which give information on the rate of convergence of $\{M_L\}$. Estimates of δ and c may be obtained by taking the limits of the sequences [20]

$$\delta_L=\frac{\log\left(|M_{L+1}-M_L|/|M_L-M_{L-1}|\right)}{\log\left(|M_L-M_{L-1}|/|M_{L-1}-M_{L-2}|\right)}, \tag{20}$$

$$c_L=\frac{|M_{L+1}-M_L|}{|M_L-M_{L-1}|^{\delta_L}}, \tag{21}$$

as $L\to\infty$. As an example, Table I shows the values of δ_L and c_L when L is comprised between 5 and 9, calculated for the considered geometrical configuration at the operating frequency of 30 MHz. As

TABLE I: Estimated OC and AEC for the sequence $\{M_L\}$.

L	δ_L	c_L
5	0.955	0.462
6	0.971	0.424
7	0.986	0.415
8	0.990	0.388
9	0.992	0.372

TABLE II: CPU time comparisons for the computation of M.

Approach	average CPU time [s]	Speed-Up
G7-K15 scheme	1.69	-
(15) with $L=2$	$3.49\cdot10^{-6}$	$4.84\cdot10^{5}$
(15) with $L=4$	$4.58\cdot10^{-5}$	$3.69\cdot10^{4}$
(15) with $L=6$	$7.26\cdot10^{-4}$	$2.33\cdot10^{3}$
(15) with $L=10$	$8.12\cdot10^{-2}$	20.8

can be observed, as L is increased the estimate δ_L of the order of convergence approaches unity, thus suggesting that the sequence of partial sums in (15) converges linearly. In addition, the small value of the asymptotic error constant contributes to accelerate the convergence of the proposed solution, since it implies a significant reduction of the remainder $M-M_L$ at any further iteration of the sequence $\{M_L\}$.

Accuracy being equal, use of (15) in place of Gauss-Kronrod scheme allows to reduce significantly the computation time. This aspect is illustrated by Table II, which shows the average CPU time taken by the two approaches to calculate the amplitude-frequency spectra of M depicted in Fig. 2. Table II also shows the ratio of the time taken by numerical integration to that required by (15), that is the speed-up exhibited by the new method. As is seen, use the new method with L=10 instead of Gauss-Kronrod scheme permits to reduce the time cost by at least 20 times.

It should be noted that (2) and, as a consequence, the developed theory, is valid subject to the condition that the current in the source coil is uniform, which, in general, is a reasonable assumption as long as the total length of the wire that constitutes the coil is less than $\lambda/3$, being λ the free-space wavelength [10]. This implies an upper limit on the frequency range of validity of (15), which, however, is always greater than the limit of validity of the quasi-static field assumption underlying the previously published approach [9]. This aspect is illustrated in Fig. 3, which depicts profiles of the amplitude of M as a function of the total wire length l_{tot} of the source coil, expressed in free-space wavelengths. The curves have been obtained by using (15), Gauss-Kronrod integration of (2) and the quasi-static approach, assuming the same two-coil system as in the preceding example. Three distinct values for the coil-to-coil spacing d are considered. As is evident from the data in Fig. 3, the exact curve arising from (15) and numerical integration of (2) starts to deviate from the quasi-static trend when $l_{tot}\cong 0.02\lambda$, that is well before the failure of the assumption of electrically small coil. The plotted curves also point out that the upper

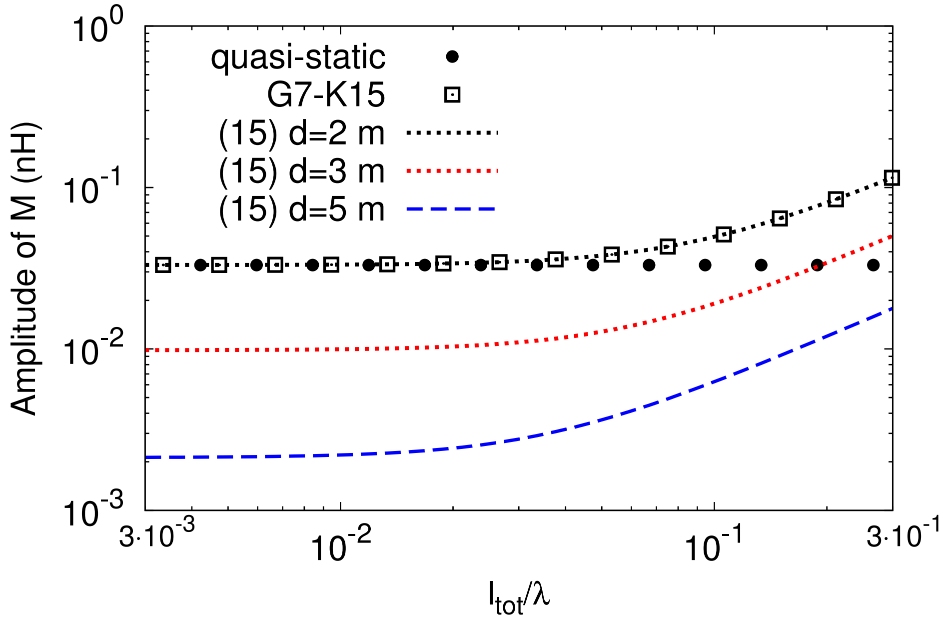

Fig. 3: Mutual inductance between two pancake coils against the total wire length l_{tot}, expressed in free-space wavelengths. Three different values for the coil-to-coil spacing are considered.

frequency limit of validity of the quasi-static assumption decreases as the distance d between the coils is increased. This is expected since, as d is increased, the frequency at which λ becomes comparable to it diminishes. The effect of changing d on the accuracy of the quasi-static solution may better understood by taking a glance at Fig. 4, which depicts $d-$profiles of $|M|$ arising from both the solution in [9] and (15). The geometrical configuration is still the same as in the previous examples, and different operating frequencies are considered. As is noticed, for small values of d the results from the quasi-static approach and (15) are overlapping, regardless of the operating frequency. Conversely, as the distance d grows up, the exact solution becomes more and more sensitive to frequency changes, and the discrepancy between any exact curve and the quasi-static trend becomes more and more pronounced. Since the data in Fig. 4 are in logarithmic scale, this implies that

$$\log\frac{|M_{(15)}|}{|M_{qs}|}{=}g\left(d\right), \tag{22}$$

where $g\left(d\right)$ is an increasing function of d. Equation (22) makes it possible to acquire information on the relative error ϵ_R arising from using the quasi-static approach instead of the proposed one. In fact, from (22) it is found that

$$\epsilon_R{=}\frac{|M_{(15)}|-|M_{qs}|}{|M_{(15)}|}{=}1-10^{-g(d)}, \tag{23}$$

which suggests us that the percent relative error generated by the quasi-static approach asymptotically approaches 100% as d grows up. This conclusion is confirmed by Fig. 5, which shows plots of the relative error against d, with the operating frequency taken as a parameter. As is seen, the slopes of the error curves are steepest for low values of d, and dramatically reduce as d is increased. Finally, they tend asymptotically to zero as soon as the error approaches unity.

IV. Conclusion

In this work, a series solution for the mutual inductance of two co-axial pancake coils is presented. Gegenbauer addition theorem and term-by-term analytical integration allow to express the mutual induc-

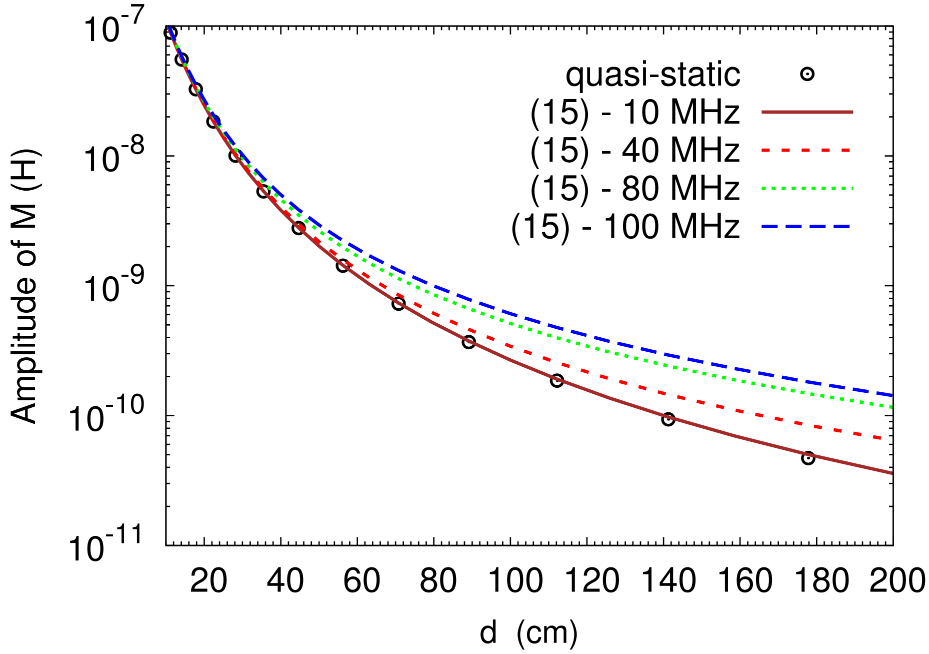

Fig. 4: Mutual inductance between two pancake coils against the axial distance d, calculated by taking the operating frequency as a parameter.

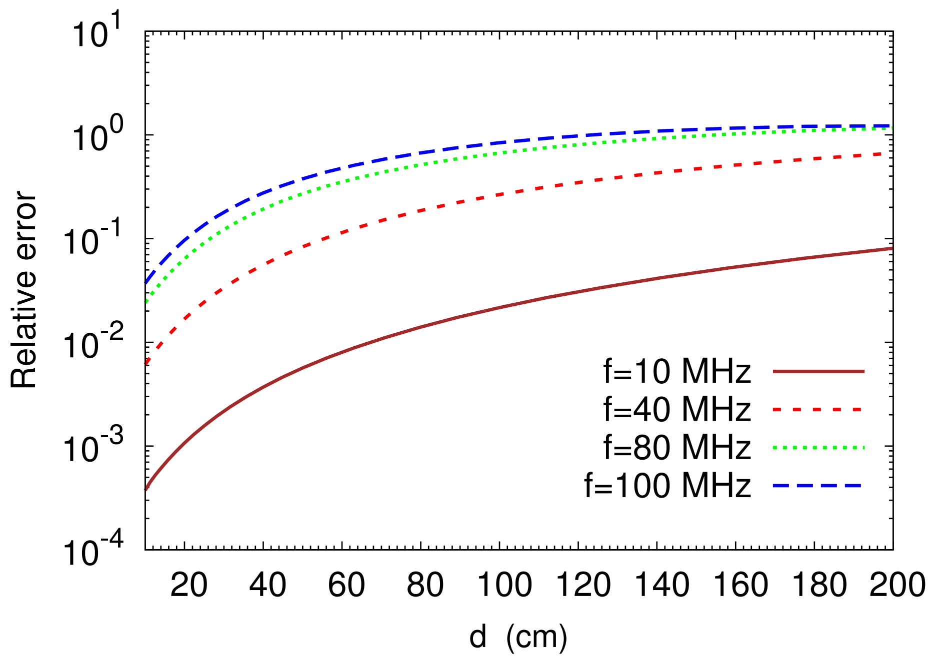

Fig. 5: Relative error of the quasi-static approximation as compared to (15), computed against d.

tance between two generic turns belonging to distinct coils as a sum of spherical Hankel functions with algebraic coefficients. Numerical tests are performed to confirm the accuracy of the proposed formula, and to illustrate its advantages in terms of computation time over standard numerical techniques that may be used to calculate the mutual inductance.

References

[1] T. Imura, H. Okabe, and Y. Hori, "Basic experimental study on helical antennas of wireless power transfer for electric vehicles by using magnetic resonant couplings," in *2009 IEEE Vehicle Power and Propulsion Conference*, Sep. 2009, pp. 936–940.

[2] Yungtaek Jang and M. M. Jovanovic, "A contactless electrical energy transmission system for portable-telephone battery chargers," *IEEE Transactions on Industrial Electronics*, vol. 50, no. 3, pp. 520–527, June 2003.

[3] C. Xiao, D. Cheng, and K. Wei, "An lcc-c compensated wireless charging system for implantable cardiac pacemakers: Theory, experiment, and safety evaluation," *IEEE Transactions on Power Electronics*, vol. 33, no. 6, pp. 4894–4905, June 2018.

[4] T. Vali, G. Marotta, L. De Santis, G. Antonini, D. Romano, and G. De Luca, "Full-wave modeling of inductive coupling links for low-power 3d system integration," in *2013 IEEE International Symposium on Electromagnetic Compatibility*, Aug 2013, pp. 17–21.

[5] L. Jianyu, T. Houjun, and G. Xin, "Frequency splitting analysis of wireless power transfer system based on t-type transformer model," *Elektronika ir Elektrotechnika*, vol. 19, no. 10, pp. 109–113, 2013.

[6] Y. Chung, T. Lee, and S. Y. Lee, "Characteristic comparison of different resonators to extend transfer distance in superconducting wireless power transfer for electric vehicle using high temperature superconducting resonance coil," *Journal of International Council on Electrical Engineering*, vol. 7, no. 1, pp. 249–254, 2017.

[7] M. Parise, "An exact series representation for the EM field from a circular loop antenna on a lossy half-space," *IEEE Antennas and Wireless Propagation Letters*, vol. 13, pp. 23–26, 2014.

[8] ——, "On the surface fields of a small circular loop antenna placed on plane stratified earth," *International Journal of Antennas and Propagation*, vol. 2015, pp. 1–8, 2015.

[9] C. M. Zierhofer and E. S. Hochmair, "Geometric approach for coupling enhancement of magnetically coupled coils," *IEEE Transactions on Biomedical Engineering*, vol. 43, no. 7, pp. 708–714, 1996.

[10] C. A. Balanis, *Antenna Theory: Analysis and Design (4th Ed.)*. New York: John Wiley & Sons, 2016.

[11] G. N. Watson, *A treatise on the theory of Bessel functions*, ser. Cambridge mathematical library. Cambridge (UK): Cambridge University Press, 1944.

[12] A. Erdelyi, *Tables of Integral Transforms*. New York: McGraw-Hill, 1954, vol. I.

[13] M. Parise and G. Antonini, "On the inductive coupling between two parallel thin-wire circular loop antennas," *IEEE Transactions on Electromagnetic Compatibility*, vol. 60, no. 6, pp. 1865–1872, 2018.

[14] I. S. Gradshteyn and I. M. Ryzhik, *Table of Integrals, Series, and Products*, A. Jeffrey and D. Zwillinger, Eds. New York: Academic Press, 2007.

[15] D. H. Werner, "An exact integration procedure for vector potentials of thin circular loop antennas," *IEEE Transactions on Antennas and Propagation*, vol. 44, no. 2, pp. 157–165, 1996.

[16] M. Parise, "Second-order formulation for the quasi-static field from a vertical electric dipole on a lossy half-space," *Progress In Electromagnetics Research*, vol. 136, pp. 509–521, 2013.

[17] ——, "Exact em field excited by a short horizontal wire antenna lying on a conducting soil," *AEU-International Journal of Electronics and Communications*, vol. 70, no. 5, pp. 676–680, 2016.

[18] ——, "Efficient computation of the surface fields of a horizontal magnetic dipole located at the air-ground interface," *International Journal of Numerical Modelling: Electronic Networks, Devices and Fields*, vol. 29, no. 4, pp. 653–664, 2016.

[19] M. Parise, M. Muzi, and G. Antonini, "Loop antennas with uniform current in close proximity to the earth: Canonical solution to the surface-to-surface propagation problem." *Progress in Electromagnetics Research B*, vol. 77, pp. 57–69, 2017.

[20] A. S. Householder, "The numerical treatment of a single nonlinear equation," 1970.